JOURNAL OF MATERIALS SCIENCE 26 (1991) 3517–3525

Mechanical properties of $Ni_3(Si, Ti)$ polycrystals alloyed with substitutional additions

TAKAYUKI TAKASUGI
Institute for Materials Research, Tohoku University, Sendai 980, Japan
MITSUHIKO YOSHIDA
Miyagi National College of Technology, Natori, Miyagi-prefecture, 981-12 Japan

The mechanical properties of the $L1_2$-type $Ni_3(Si, Ti)$ polycrystals, which were alloyed with 1–2 at% of various transition metals and also doped with boron, were investigated over a wide range of temperatures. The addition of Hf enhanced the levels of yield stress whereas the addition of Cr, Mn and Fe reduced the levels of the yield stress over a wide range of temperatures. $Ni_3(Si, Ti)$ alloyed with Cr, Mn and Fe showed a shallow minimum in the yield stress–temperature curves. This result was correlated with the modification of the micro-cross-slip process by the additives. At low temperatures, the addition of Hf and Nb slightly reduced the elongation, while the addition of Cr, Mn and Fe improved elongation. This elongation behaviour was interpreted as the alloying effect on the intergranular cohesive strength of $L1_2$ ordered alloys. At high temperatures, the elongation of $Ni_3(Si, Ti)$ alloyed with Hf showed a particularly high value. This elongation behaviour is discussed based on the alloying effect on the competition between dynamic recrystallization and cavitation at grain boundaries. The fracture surfaces exhibited a variety of fracture patterns, depending on temperature and the alloy, and were primarily well correlated with the elongation behaviour. The ductilities of most of the alloys at high temperatures were reduced by the tests in air.

1. Introduction

$Ni_3(Si, Ti)$ alloys with $L1_2$ structure have unique strength and ductility properties. As shown in Fig. 1, it was reported that $Ni_3(Si, Ti)$ alloys exhibited an increase in flow strength with increasing temperature and also displayed high ductility over a wide range of test temperatures [1, 2]. In particular, its strength level was extremely high compared to other $L1_2$ ordered alloys which are being developed as advanced materials. $Ni_3(Si, Ti)$ alloys were also shown to have an excellent corrosion resistance in H_2SO_4 and oxidation resistance in air, at ambient and elevated temperatures, respectively [3]. Thus, these alloys are considered to be candidate alloy systems which could be used as high-temperature structural materials or chemical parts.

To try to improve the mechanical property of the $Ni_3(Si, Ti)$ alloys, a small amount of interstitial atoms or small diameter atoms was added [1, 2, 4]. The addition of B [1, 2] and C [4] improved the ductility, while the addition of the Be [4] moderately enhanced the strength. An improvement in the mechanical properties of $Ni_3(Si, Ti)$ alloys may also be achieved by the technique of macro-alloying. In this work, the mechanical properties of $Ni_3(Si, Ti)$ polycrystals alloyed with various transition metals are reported. The strength, elongation and fracture behaviour of these quarternary $Ni_3(Si, Ti)$ alloys were investigated by tensile tests over a wide range of testing temperatures. Emphasis is placed on clarifying the alloying effect, the grain size effect, the temperature dependence and the test environmental effect. The micro-mechanisms associated with the phenomena observed in this work are not dealt with in this paper

2. Experimental procedure

The base composition of the $Ni_3(Si, Ti)$ alloys used in this work was 79.5 at % Ni, 11 at % Si and 9.5 at % Ti and located in a single-phase region of the $L1_2$ structure [5]. This composition was identical to that of unalloyed $Ni_3(Si, Ti)$, the mechanical properties of which were previously reported [2, 6]. Table I shows the additives selected in this work. The alloying behaviour (whether the additives substitute for Ni, Si or both) and their solubility limits in Ni_3Si alloy have been summarized from the ternary phase diagram [7]. Based on these results, 1 at % Hf, Nb, Cr and Mn, and 2 at % Fe were added to substitute for the constituent element, Ti.

The starting materials were 99.9 wt % Ni, 99.999 wt % Si, 99.8 wt % Ti, 95 wt % Hf (the remaining element was mostly Zr), 99.5 wt % Nb, 99.99 wt % Cr, 99.9 wt % Mn and 99.9 wt % Fe. All of the alloy

0022–2461/91 $03.00 + .12

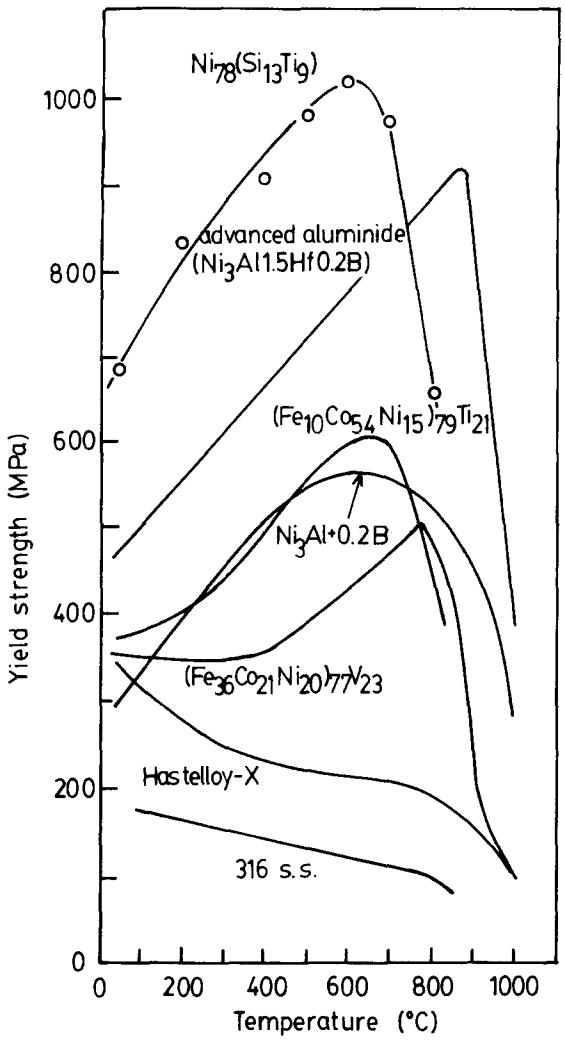

Figure 1 Variations of the yield stresses for some $L1_2$ ordered alloys and conventional alloys with temperature.

systems selected in this work were doped with about 0.004 wt % B, using the master alloy of Ni–10 wt % B. The B-doping was conducted to enhance the ductility of these alloys and also to suppress the environmental embrittlement associated with H_2 at ambient temperatures [2, 4, 6]. The alloy buttons were prepared by nonconsumable arc melting in an argon atmosphere. The nominal and analysed chemical compositions of the alloys used in this work are shown in Table II; an agreement between two values was fairly good for each element.

The alloy buttons in the form of the square rod (approximately 15 mm × 15 mm × 80 mm) were homogenized at 1323 K for 1 day in vacuum. These buttons were then worked to plates of about 1 mm thickness by repeated rolling (at 573 K in air)/annealing (at 1273 K in vacuum). The annealing for recrystallization was mostly done at 1273 K for 5 h in vacuum. To observe the grain size effect on the mechanical property of the $Ni_3(Si, Ti)$ alloyed with Nb, annealing was also performed at 1173 K for 5 h in vacuum.

Metallographic examination and X-ray diffraction (XRD) measurements were performed to characterize the microstructures of these alloys, using their plate specimens which were electrolytically polished in a solution of 20% H_2SO_4 and 80% CH_3OH. Higher index lines of (2 2 0) were used to determine the lattice parameter of the $L1_2$ phase.

The tensile specimens with dimensions of approximately 1.2 mm × 2.2 mm × 14 mm gauge length were prepared by a precision wheel cutter and an electro-erosion machine. The faces of the specimens were abraded on SiC paper. The tensile tests were carried out using an Instron testing machine at a nominal strain rate of $1.2 \times 10^{-3}\ s^{-1}$. The testing temperatures

TABLE I Microstructures of the $Ni_3(Si, Ti)$ alloyed with various additives

Additive	Amount (at %)	Structure		Lattice parameter (nm)	Grain size (μm)
		OM[a]	XMD[b]		
Hf (IVa)	1	$L1_2$ + X[c]	$L1_2$ + X	0.3552	17
Nb (Va)	1	$L1_2$	$L1_2$	0.3553	45 (16)
Cr (VIa)	1	$L1_2$	$L1_2$	0.3550	26
Mn (VIIa)	2	$L1_2$	$L1_2$	0.3548	32
Fe (VIII)	1	$L1_2$ + X	$L1_2$	0.3548	23

[a] Observation by optical microscopy.
[b] Measurement by X-ray diffractometry.
[c] The second phase.

TABLE II Chemical composition of $Ni_3(Si, Ti)$ alloys used in this work

Alloy	Nominal (analysed) composition				
	Ni (at %)	Si (at %)	Ti (at %)	Additives (at %)	Boron (wt %)
$Ni_3(Si, Ti, Hf)$	79.5(–)	11(10.35)	8.5(8.58)	1(0.92)	0.004(0.0033)
$Ni_3(Si, Ti, Nb)$	79.5(–)	11(10.39)	8.5(8.61)	1(0.99)	0.004(0.0036)
$Ni_3(Si, Ti, Cr)$	79.5(–)	11(10.61)	8.5(8.52)	1(1.04)	0.004(0.0032)
$Ni_3(Si, Ti, Mn)$	79.5(–)	11(10.48)	7.5(7.56)	2(1.92)	0.004(0.0030)
$Ni_3(Si, Ti, Fe)$	79.5(–)	11(10.56)	8.5(8.62)	1(0.79)	0.004(0.0029)

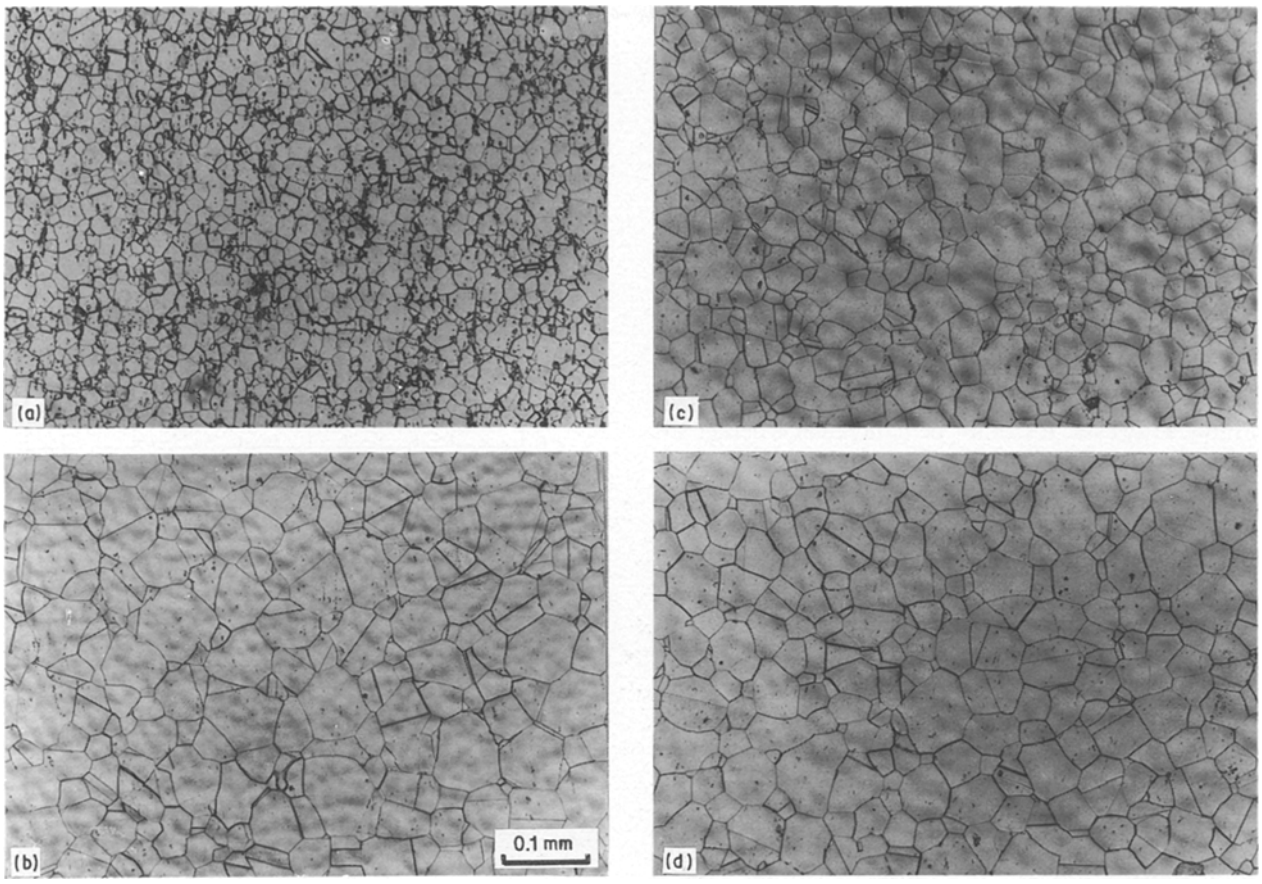

Figure 2 Optical microstructures of various $Ni_3(Si, Ti, X)$ alloys (X = the additives) observed in this work. (a) 1 Hf, (b) 1 Nb, (c) 1 Cr, (d) 2 Mn, (e) 1 Fe.

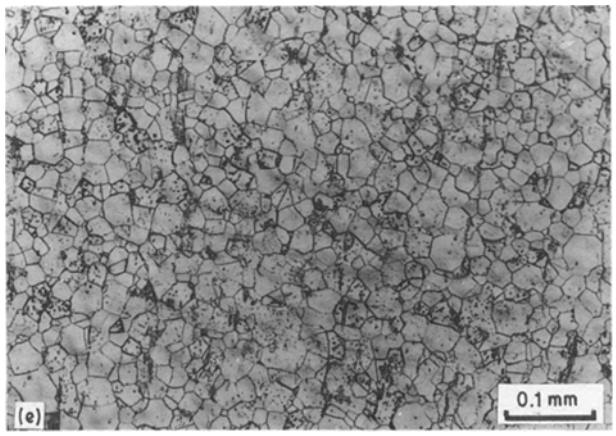

were from 77–1073 K. The tests at 77 K were performed with an apparatus suspended in a Dewar vessel filled with liquid nitrogen. The tensile tests at room temperature and at elevated temperatures were conducted in a vacuum (better than 1.3×10^{-3} Pa). To observe the environmental effect, the tensile tests at room temperature and at 673 K were also performed in air. After tensile testing, the fracture surfaces of the specimens were examined by scanning electron microscopy (SEM).

3. Results

3.1. Microstructures

Fig. 2 shows the optical microstructures of various $Ni_3(Si, Ti, X)$ alloys (where X represents the additives) observed in this work. These photographs clearly show that $Ni_3(Si, Ti)$ alloyed with Nb, Cr and Mn consisted of a single phase with $L1_2$ structure while $Ni_3(Si, Ti)$ alloyed with Hf and Fe contained second-phase particles. The former alloys showed larger grain sizes than the latter alloys (the grain sizes measured by the simple intercept method are shown in Table I). This difference reveals that grain growth during annealing in the latter alloys was retarded by the second-phase particles.

In the XRD measurements, peaks from the second-phase particles were detected in $Ni_3(Si, Ti)$ alloyed with Hf, corresponding to the results from optical microscopy. However, these were not detected in $Ni_3(Si, Ti)$ alloyed with Fe, and is thus inconsistent with results of optical microscopy. The lattice parameters of the $L1_2$ phase in various $Ni_3(Si, Ti, X)$ alloys are shown in Table I and are almost identical to the unalloyed $Ni_3(Si, Ti)$, i.e. 0.355 05 nm [5], revealing that the additives selected in this work were small or beyond the solubility limits, and therefore had no effect on the lattice parameters.

3.2. Tensile properties

Tensile properties of $Ni_3(Si, Ti, X)$ alloys observed in this work are described in two different groups because the additives of Hf(IVa) and Nb(Va) produced somewhat different results from those of Cr(VIa), Mn(VIIa) and Fe(VIII).

3.2.1. Tensile properties of $Ni_3(Si, Ti)$ alloyed with Hf and Nb

The variation in yield stress (defined as an offset stress of 0.2% plastic strain) with temperature for each alloy is shown in Fig. 3, together with that for the unalloyed $Ni_3(Si, Ti)$ which has similar grain size and was tested under similar experimental conditions [2]. The yield stress–temperature curves are similar; the yield stress began to increase from 77 K with increasing temperature, reached a maximum and then decreased rapidly with further increasing temperature.

The yield stress of the $Ni_3(Si, Ti)$ alloy was enhanced by the addition of Hf at almost all test temperatures. However, it cannot be concluded whether the solution hardening by solute atoms, Hf or the precipitation hardening by the second phase particles is dominantly responsible for the enhanced strength. On the other hand, the yield stress of $Ni_3(Si, Ti)$ alloys was not actually affected by the addition of Nb but was slightly reduced particularly at temperatures above room temperature. Here, it must be remembered that the grain size of this alloy was larger than those of the other alloys as shown in Table I. To explain this result, the grain size effect on the mechanical properties of this alloy will be observed in a later section.

Fig. 4 illustrates the variations of elongation (Fig. 4a) and ultimate tensile stress (UTS) (Fig. 4b) with temperature for each alloy. These data were taken from the tensile tests under vacuum. The two $Ni_3(Si, Ti)$ alloyed with Hf and Nb basically showed similar curves to that of the unalloyed $Ni_3(Si, Ti)$. However, the elongation of two quarternary alloys showed higher values at 77 K, lower values at medium temperatures (between 300 and 673 K), and higher values at high temperatures (above 873 K) than the unalloyed $Ni_3(Si, Ti)$. Here, an interesting result is that the elongation values of $Ni_3(Si, Ti)$ alloyed with Hf were much higher at high temperatures than the other two alloys and also tended to increase at the highest temperature tested (1073 K). The UTS of $Ni_3(Si, Ti)$ alloyed with Hf was higher at high temperatures than for the other two alloys.

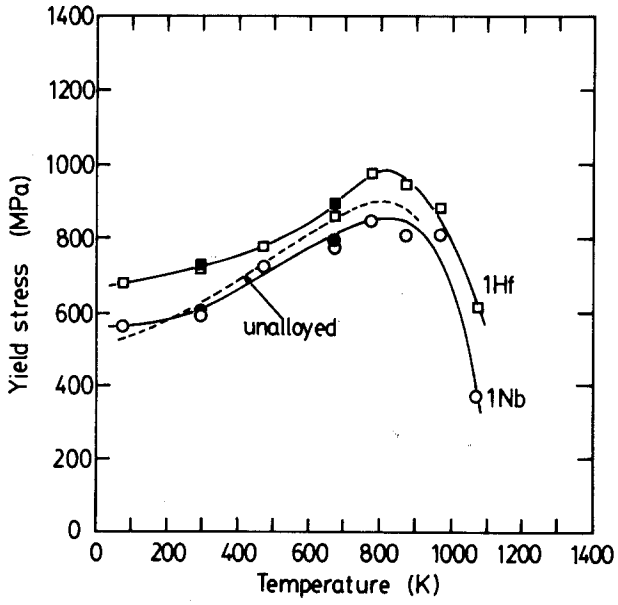

Figure 3 Variations of the 0.2% yield stress of $Ni_3(Si, Ti, Hf)$ and $Ni_3(Si, Ti, Nb)$ alloys with temperature, tested in (○, □) vacuum and (●, ■) air. The data for unalloyed $Ni_3(Si, Ti)$ are included for comparison.

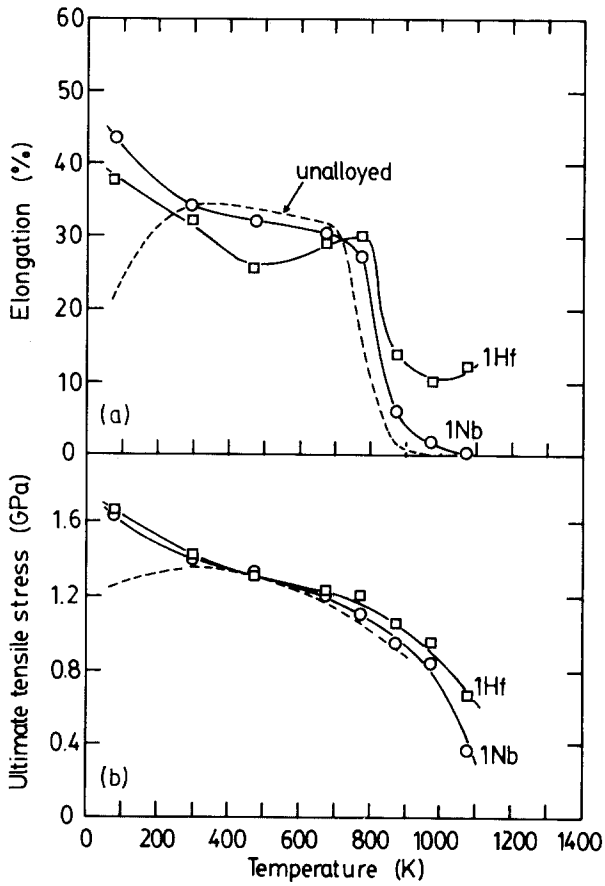

Figure 4 Variations of (a) elongation and (b) ultimate tensile stress (UTS) of $Ni_3(Si, Ti, Hf)$ and $Ni_3(Si, Ti, Nb)$ alloys with temperature. These data were taken from the tests in vacuum. The data for unalloyed $Ni_3(Si, Ti)$ are included for comparison.

Figs 5, 6a and b show the grain size effect on the yield stress, the elongation and UTS of $Ni_3(Si, Ti)$ alloyed with Nb, respectively. The data (in Fig. 3) taken from the specimens with a grain size of 45 μm were compared with data taken from the specimens with a grain size of 16 μm. These figures clearly show that the specimens with smaller grain size enhanced all values of yield stress, elongation and UTS over a wide range of test temperatures and also showed larger values than that of the unalloyed $Ni_3(Si, Ti)$.

Figs 7 and 8 show the variations of the fractographic patterns observed in $Ni_3(Si, Ti)$ alloyed with Hf and Nb with temperature, respectively. For both alloys, the transgranular fractures with dimple-like patterns was dominant at temperatures up to 673 K, and the intergranular fracture patterns became more dominant at temperatures above 873 K. For $Ni_3(Si, Ti)$ alloyed with Nb, the intergranular fracture mode was more significant at high temperatures than in $Ni_3(Si, Ti)$ alloyed with Hf. A comparison of the fractography at 1073 K between two alloys at high magnification is represented in Fig. 9. The fracture pattern of either alloy apparently consisted of grain-boundary facets. However, the fracture patterns of

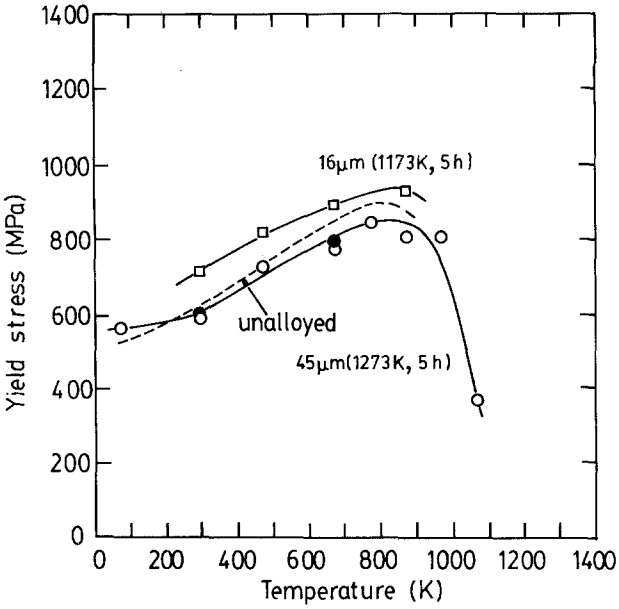

Figure 5 Variations of yield stress of $Ni_3(Si, Ti, Nb)$ alloys with temperature, showing the effect of the grain size. These data were taken from the tests in vacuum.

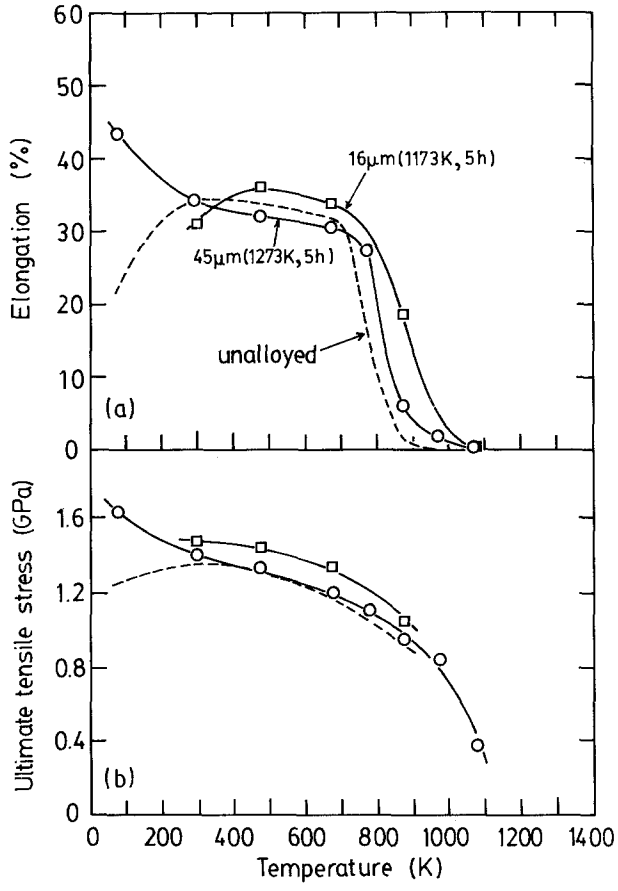

Figure 6 Variations of (a) elongation and (b) ultimate tensile stress (UTS) of $Ni_3(Si, Ti, Nb)$ alloys with temperature, showing the grain size effect. These data were taken from the tests in vacuum. The data for unalloyed $Ni_3(Si, Ti)$ are included for comparison.

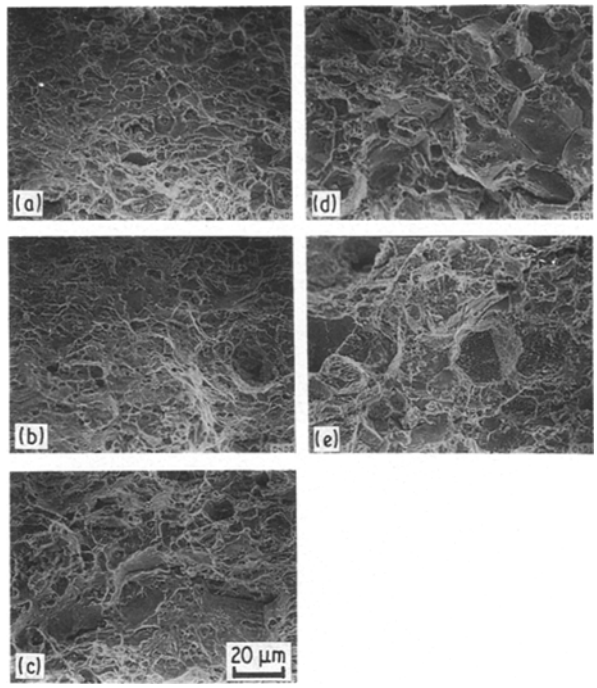

Figure 7 Variation of the fracture patterns of $Ni_3(Si, Ti, Hf)$ alloys with temperature. The tests were performed in vacuum. (a) 300 K, (b) 473 K, (c) 673 K, (d) 873 K, (e) 1073 K.

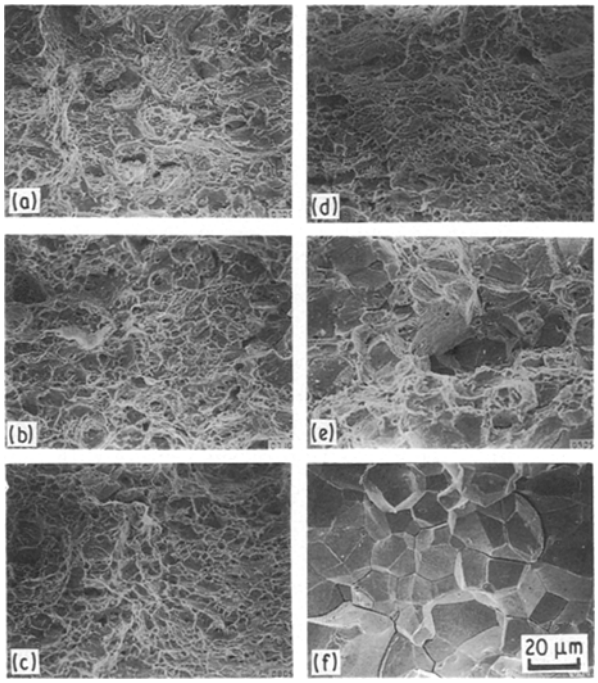

Figure 8 Variation of fracture patterns of $Ni_3(Si, Ti, Nb)$ alloys with temperature. The tests except 77 K were performed in vacuum. (a) 77 K, (b) 300 K, (c) 473 K, (d) 673 K, (e) 873 K, (f) 1073 K.

$Ni_3(Si, Ti)$ alloyed with Hf showed more ductile fracture patterns, i.e. a number of dynamically recrystallized grains on these facets. This result suggests that the higher elongation value obtained at the highest temperature (1073 K) in $Ni_3(Si, Ti)$ alloyed with Hf (see Fig. 4) may be attributed to dynamic recrystallization.

Thus, the fracture surfaces of the tensile specimens exhibited a variety of fracture patterns, depending on the temperature and the alloy. However, the fracture patterns were primarily correlated with the elongation. In the specimens showing higher elongation values, transgranular fracture patterns were dominant.

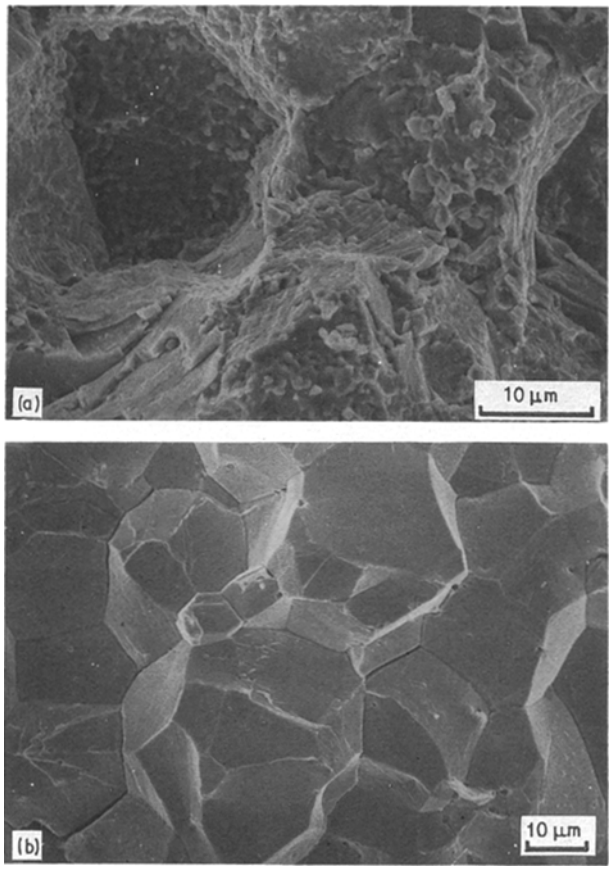

Figure 9 Fracture patterns taken at high magnification of (a) $Ni_3(Si, Ti, Hf)$ and (b) $Ni_3(Si, Ti, Nb)$ alloys tensile-tested at 1073 K, in vacuum.

3.2.2. Tensile properties of $Ni_3(Si, Ti)$ alloyed with Cr, Mn and Fe

The variation of yield stress with temperature for each alloy is shown in Fig. 10. The yield stress–temperature curves in this group were similar but differed from those of unalloyed $Ni_3(Si, Ti)$ [2] and also from those of alloys in the former group; the yield stresses displayed a shallow minimum around room temperature, and increased from this temperature with decreasing temperature. This variation of yield stress with temperature has been observed for Co_3Ti alloys [8] and Pt_3Al alloys [9].

The yield stresses of the $Ni_3(Si, Ti, X)$ alloys in this group were slightly enhanced at 77 K but reduced at high temperatures by the addition of X.

Fig. 11 illustrates the variations of elongation (Fig. 11a) and UTS (Fig. 11b) with temperature for each alloy. These data were again taken from the tensile tests in vacuum. These alloys basically displayed similar curves of elongation versus temperature to that of the unalloyed $Ni_3(Si, Ti)$. However, it is noted that the elongation of the alloys in this group showed higher values at almost all test temperatures. In particular, this improvement was remarkable at 77 K and at high temperatures, above 773 K. Small peaks appeared around at 773 K. However, these alloys did not show the increase in elongation at sufficiently high temperature (1073 K), in contrast to $Ni_3(Si, Ti)$ alloyed with Hf. On the other hand, the UTS of $Ni_3(Si, Ti)$ alloyed with these additives were

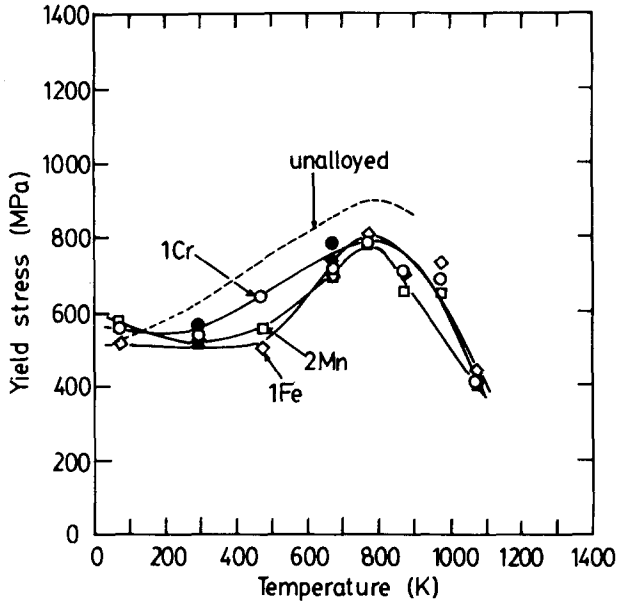

Figure 10 Variations of yield stress of $Ni_3(Si, Ti, X)$ (X = Cr, Mn and Fe) alloys with temperature, tested in (○, □, ◇) vacuum and (●, ◆) air. The data for unalloyed $Ni_3(Si, Ti)$ are included for comparison.

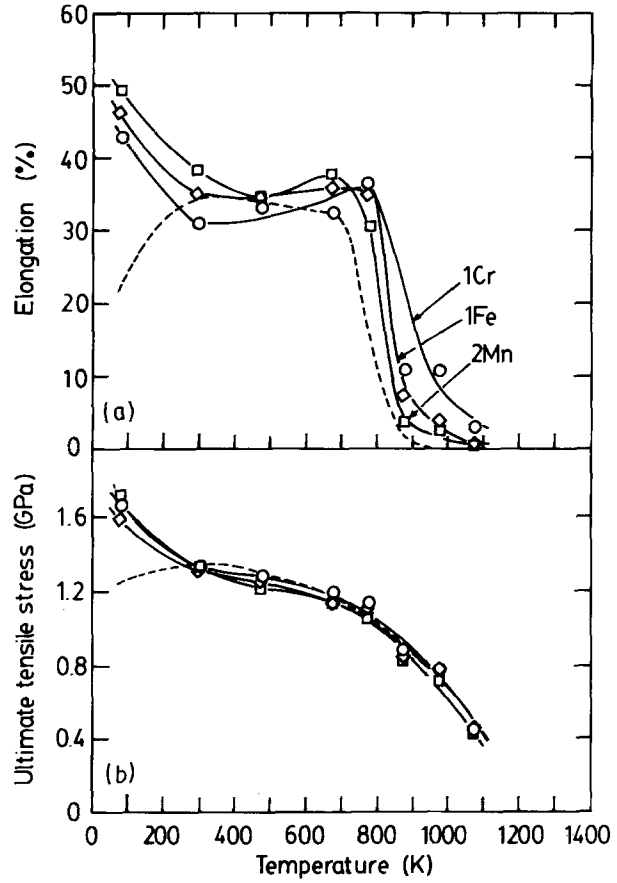

Figure 11 Variations of (a) elongation and (b) ultimate tensile stress (UTS) of $Ni_3(Si, Ti, X)$ (X = Cr, Mn and Fe) alloys with temperature. These data were taken from tests in vacuum. The data for unalloyed $Ni_3(Si, Ti)$ are included for comparison.

higher at 77 K than in the unalloyed $Ni_3(Si, Ti)$ and then were almost identical to the unalloyed $Ni_3(Si, Ti)$ at remaining temperatures.

As a representative of the alloys in this group, Fig. 12 shows the variation of fractographic patterns

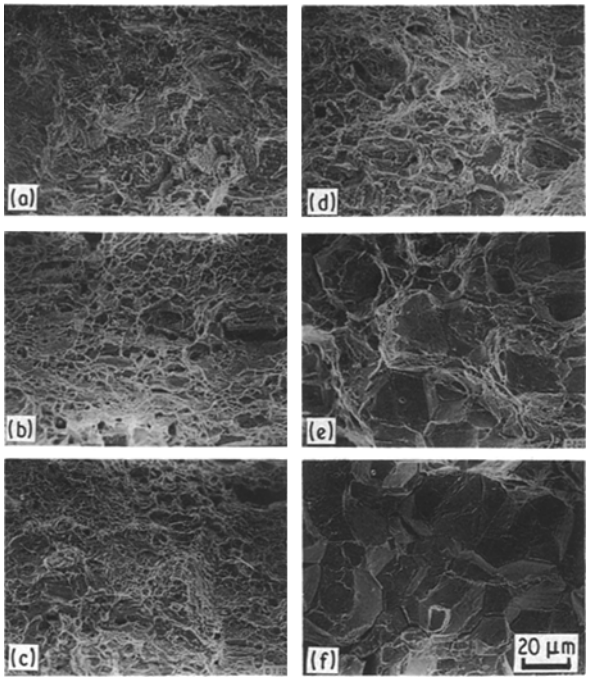

Figure 12 Variation of the fracture patterns of $Ni_3(Si, Ti, Cr)$ alloys with temperature. The tests except 77 K were performed in vacuum. (a) 77 K, (b) 300 K, (c) 473 K, (d) 673 K, (e) 873 K, (f) 1073 K.

for $Ni_3(Si, Ti, Cr)$ alloys with temperature. The transgranular fractures with dimple-like patterns were predominant at low temperatures, while the intergranular fracture patterns became more dominant at high temperatures. The fractographs at 1073 K in this alloy and also the remaining two alloys showed relatively smooth grain-boundary facets, suggesting little occurrence of the dynamic recrystallization. Thus, the fractographs observed in these $Ni_3(Si, Ti, X)$ alloys correlate well with the elongation behaviour in terms of temperature and alloying element.

3.2.3. Environmental effect on the mechanical property

The previous observation indicated that $Ni_3(Si, Ti)$ alloys and B-doped $Ni_3(Si, Ti)$ alloys were very sensitive to hydrogen embrittlement operating at ambient temperatures and to oxygen embrittlement operating at elevated temperatures, respectively [6]. Therefore, tensile tests in air were also performed in this work. Room temperature and 673 K were selected as test temperatures at which to investigate this effect.

The yield stresses taken from the tests in air are plotted in Figs 3, 5 and 10 for each alloy and are shown to be basically identical to those obtained in vacuum, not only at room temperature but also at 673 K. Thus, it is evident that the yield stress in all the alloy systems observed in this work was little affected by the environmental medium.

Fig. 13 summarizes the environmental effect on the elongations at room temperature (Fig. 13a) and at 673 K (Fig. 13b). The environmental effect at room temperature for the $Ni_3(Si, Ti, X)$ alloys was similar to unalloyed $Ni_3(Si, Ti)$ containing 50 p.p.m. B [6]; no losses of elongation in air were observed for these

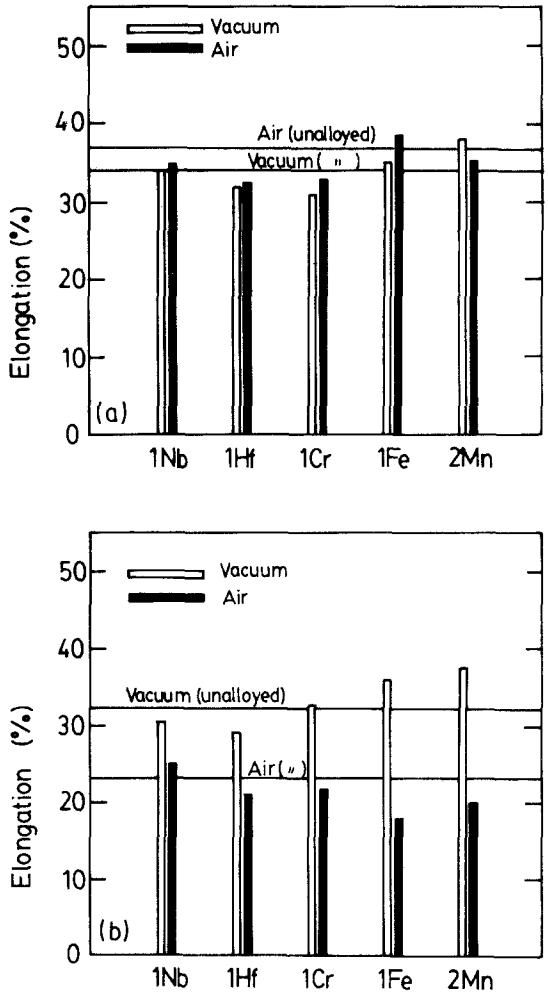

Figure 13 Environmental effect on elongation of $Ni_3(Si, Ti, X)$ alloys at (a) room temperature and (b) 673 K.

alloys. This implies that small amounts of B (40–50 p.p.m.) contained in these alloys suppressed the action of H_2 penetrating from the air as the B atom in the unalloyed $Ni_3(Si, Ti)$ did [6]. The present experiment also indicates that no substitutional additive atoms affected this phenomenon, i.e. they did not induce hydrogen embrittlement.

On the other hand, an environmental effect at 673 K for $N_3(Si, Ti, X)$ alloys was clearly recognized, as observed in unalloyed $Ni_3(Si, Ti)$ containing the 50 p.p.m. B [6]. This implies that small amounts of B (40–50 p.p.m.) contained in these alloys introduced the action of oxygen penetration from air, as did the boron atom in unalloyed $Ni_3(Si, Ti)$ [6]. Thus, no additives suppressed the oxygen-related environmental embrittlement in $Ni_3(Si, Ti)$ alloys containing B. Rather, it is seen in Fig. 13b that the additives of Fe and Mn greatly accelerated oxygen embrittlement of $Ni_3(Si, Ti)$ alloys.

4. Discussion

It has been proposed that the yield stress–temperature curve in the $L1_2$ ordered alloys should be regarded as the sum of three temperature-dependent terms and the yield stress, σ_y, can be expressed as

$$\sigma_y = \sigma_{ath} + \sigma(I)_{th} + \sigma(II)_{th} \quad (1)$$

The stress component of the first term in this equation has an ordinary negative temperature dependence of stress, arising from shear modulus change with temperature and correlated with the solid solution hardening by the additives. The second and third terms correspond to the (anomalous) "negative" temperature and "positive" temperature dependence of the stress which were dominantly operative at low and high temperatures, respectively.

The effect of the additives on the yield stress of $Ni_3(Si, Ti)$ alloys could be discussed based on these terms. The result showed that the addition of Hf enhanced the yield stress, particularly at low temperatures, whereas the addition of Nb, Cr, Mn or Fe slightly enhanced the yield stress at 77 K. This strengthening behaviour is related to the σ_{ath} term associated with the solution hardening. If we assume that this strengthening is primarily due to the size difference between the constituent atom, Ti (or Si) and the additive, X, a larger strengthening can be expected on the addition of Hf, whereas this can be moderate for additions of Nb, Cr, Mn and Fe. A large misfit of atomic diameter exists between Ti ($r = 0.147$ nm) (or Si, ($r = 0.117$ nm)) and Hf ($r = 0.160$ nm). On the other hand, the misfits of atomic diameter between Ti (or Si) and Nb ($r = 0.143$ nm), (Ti (or Si) and Cr ($r = 0.125$ nm), Ti (or Si) and Mn ($r = 0.150$ nm), and Ti (or Si) and Fe ($r = 0.124$ nm)) are not so large. However, the elastic interaction term must be included in the more quantitative evaluation of this.

The large reduction in yield stress of $Ni_3(Si, Ti)$ alloyed with Cr, Mn and Fe at temperatures above room temperature could be attributed to the modification of $\sigma(II)_{th}$ on the alloying; Mishima *et al.* [10] predicted, based on the phase stability concept, that when atoms located near Ni (i.e. group VIII elements) in the periodic table substitute for X atoms in Ni_3X alloy (where X is a b-subelement), the micro-cross-slip of a superdislocation on $\{1\,1\,1\}$ to $\{0\,0\,1\}$ is suppressed by these additives through the modification of the core structure of the superdislocation, resulting in a decrease of flow strength in this temperature regime. On the other hand, the occurrence of a negative temperature dependence of yield stress of $Ni_3(Si, Ti)$ alloyed with these elements at temperatures below room temperature could also be associated with the modification of the core structure of the superdislocation. However, more quantitative evaluation of these is, at present, impossible because the data points are scarce in this temperature regime.

For the alloying effect on elongation at ambient temperatures, where the ductility is assumed to be controlled directly by the grain-boundary cohesive strength, the addition of Hf and Nb reduced the ductility whereas the addition of Cr, Mn and Fe enhanced the ductility. It appears that the results obtained are consistent with the model proposed previously [11, 12]; the $L1_2$ ordered alloy, consisting of two transition metal elements with a similar electrochemical nature, is expected to have a homogeneous electronic distribution at the grain boundary, resulting in a higher grain-boundary cohesion and lowering the propensity for grain-boundary fracture. This led to the prediction that partial replacement of Si with Ti in the Ni_3Si alloy reduced the difference in the electrochemical bonding nature, resulting in an improvement in elongation [1, 2]. Furthermore, this prediction indicates that a partial replacement of Ti with T′(= electronically more similar element to Ni than Ti) further improves the elongation. Thus, the addition of Cr(VIa), Mn(VIIa) and Fe(VIII), the electronic natures of which are closer to Ni(VIII) element, improved the ductility of the $Ni_3(Si, Ti)$ alloys.

For the alloying effect on the elongation at high temperatures, all additives selected in this work more or less improved the ductility of the $Ni_3(Si, Ti)$ alloys. In this temperature regime, the elongation is assumed to be influenced by the competition between two counter processes of the grain-boundary cavitation and grain-boundary migration. The latter process is associated with dynamic recrystallization. Either process is controlled by the diffusion. Probably, most of the additives selected in this work enhanced the diffusion and thereby promoted grain-boundary migration. Here, it must be pointed out that the addition of Hf clearly showed evidence of dynamic recrystallization and then produced a high elongation value at high temperatures. In this case, it is very likely that second-phase particles played an important role through offering easier nucleation sites for dynamic recrystallization. However, $Ni_3(Si, Ti)$ alloyed with Fe contained second-phase particles but did not show the propensity for dynamic recrystallization, and therefore did not display a high elongation value. This implies that the size, density, morphology and coherency with the matrix of the second-phase particles must be taken into consideration for the nucleation sites of recrystallization. More detailed observation is thus required for an interpretation for high-temperature ductility.

Concerning environmental embrittlement, no substitutional element showed a beneficial effect by which the hydrogen-related embrittlement operative at low temperatures and the oxygen-related embrittlement operative at high temperatures, are suppressed. However, further studies on this subject are required using $Ni_3(Si, Ti)$ alloyed with the remaining transition elements and b-subgroup elements, before any conclusion can be drawn.

5. Conclusions

The mechanical properties of the $L1_2$-type $Ni_3(Si, Ti)$ polycrystals, which were alloyed with 1–2 at % transition metals (Hf, Nb, Cr, Mn and Fe) and also doped with about 40 p.p.m. B, were investigated at temperatures from 77–1073 K. The following results were obtained.

1. The $Ni_3(Si, Ti)$ alloyed with Nb, Cr and Mn consisted of a single phase, while that alloyed with Hf and Fe contained second-phase particles.

2. The addition of Hf enhanced the levels of the yield stress over a wide range of temperatures whereas the additions of Cr, Mn and Fe reduced the levels of the yield strength at high temperatures. Also, $Ni_3(Si, Ti)$ with Cr, Mn and Fe created a shallow

minimum in the yield stress–temperature curves. The strength behaviour at low temperatures was interpreted in terms of the solid solution hardening, while the strength behaviour at high temperatures was discussed as the modification of the micro-cross-slip process of the superdislocation by the alloying.

3. The addition of Hf and Nb slightly reduced the elongation at low temperatures but improved it at high temperatures, whereas the addition of Cr, Mn and Fe improved the elongation over all the test temperatures. The elongation behaviour observed at ambient temperature was interpreted by the alloying effect on the intergranular cohesive strength of $L1_2$ ordered alloys. The elongation behaviour at high temperatures was discussed based on the effect of alloying on the competition between the dynamic recrystallization and cavitation at grain boundaries.

4. The fracture surfaces exhibited a variety of fracture patterns, depending on temperature and the alloy, and were primarily correlated with the elongation itself. As the elongation value increased, the fracture pattern changed from intergranular to transgranular. The ductilities of most of the alloys at high temperatures were reduced by the tests in air.

Acknowledgements

This research was partly supported by a Grant-in-Aid for Scientific Research on Priority Areas, New Functionality Materials – Design, Preparation and Control, The Ministry of Education, Science and Culture. The authors thank Professor Emeritus, Tohoku University, O. Izumi, for his encouragement.

References

1. T. TAKASUGI, M. NAGASHIMA and O. IZUMI, *Acta Metall. Mater.* **38** (1990) in press.
2. T. TAKASUGI, O. IZUMI and M. YOSHIDA, *J. Mater. Sci.* **26** (1991) 1173.
3. S. HASEGAWA, T. TAKASUGI and O. IZUMI, to be published.
4. T. TAKASUGI and M. YOSHIDA, *J. Mater. Sci.* **26** (1991) 3032.
5. T. TAKASUGI, D. SHINDO, O. IZUMI and M. HIRABAYASHI, *Acta Metall.* **38** (1990) 1417.
6. T. TAKASUGI, H. SUENAGA and O. IZUMI, *J. Mater. Sci* **26** (1991) 1179.
7. S. OCHIAI, Y. OYA and T. SUZUKI, *Acta Metall.* **32** (1984) 289.
8. T. TAKASUGI, S. HIRAKAWA, O. IZUMI, S. ONO and S. WATANABE, *ibid.* **35** (1987) 2015.
9. D. M. WEE, D. P. POPE and V. VITEK, *ibid.* **32** (1984) 829.
10. Y. MISHIMA, S. OCHIAI, M. YODOGAWA and T. SUZUKI, *Trans. JIM* **27** (1986) 41.
11. O. IZUMI and T. TAKASUGI, in "Proceedings of the MRS Symposium on High-Temperature Ordered Intermetallic Alloys II", Pittsburgh, edited by N. S. Stoloff, C. C. Koch, C. T. Liu and O. Izumi, Vol. 81 (1987) pp. 173–82.
12. *Idem., J. Mater. Res.* **3** (1988) 426.

Received 26 March
and accepted 10 October 1990